RSC Advances

PAPER

View Article Online
View Journal | View Issue

Cite this: *RSC Adv.*, 2018, **8**, 16897

Room-temperature hydrogen sensing performance of Nb_2O_5 nanorod arrays

Yanan Zou,[ab] Jing He,[b] Yongming Hu,*[b] Rui Huang,[b] Zhao Wang[b] and Qibin Gu*[c]

Received 16th March 2018
Accepted 27th April 2018

DOI: 10.1039/c8ra02329h

rsc.li/rsc-advances

Nb_2O_5 nanorod arrays with a hexagonal phase were *in situ* grown on Nb foil *via* a facile hydrothermal method. The aspect ratio and spacing of the Nb_2O_5 nanorods increased upon an increase in the reaction temperature. A pair of platinum electrodes was deposited on the surface of the Nb_2O_5 nanorod arrays to form a hydrogen sensor. The sensor based on Nb_2O_5 nanorod arrays exhibited a fast and highly-sensitive hydrogen response with a sensitivity of 74.3% and a response time of 28 s toward 6000 ppm of H_2 at room temperature. The Nb_2O_5 nanorod arrays also showed good selectivity of H_2 against C_2H_6O, CO and NH_3. The hydrogen sensing performance can be attributed to the reaction between chemisorbed oxygen species and H_2. The Nb_2O_5 nanorods have a high aspect ratio, leading to an increase in the chemisorbed oxygen species on the surface of the [001] orientated nanorods. Moreover, arrays with a vertical structure have low quantities of junctions, which allow oxygen ions to diffuse more easily.

Introduction

It is widely believed that hydrogen (H_2) will be one of the most promising clean, renewable, and commonly available fuels for the future to allow critical problems such as shortages of fossil fuel resources, global warming and air pollution to be solved.[1] Unfortunately, hydrogen gas is difficult for humans to detect because it is tasteless, colorless and odorless, while its inflammable and explosive nature mean that it requires special handling.[2] Therefore, hydrogen sensors are required for monitoring hydrogen concentration and detecting its leakage and diffusion.

Nanostructured materials with a high surface-to-volume ratio are ideal for gas sensing, since gas sensing is inherently a surface phenomenon. There have been many reports on the gas sensing properties of nanostructured metal oxides, such as ZnO_2, TiO_2 and SnO_2.[3–8] However, gas sensors based on Nb_2O_5, an important semiconductor oxide with superior photocatalyst, gas sensing, electrochromic and biocompatibility properties[9–13] due to its thermodynamically stability, chemical inertness and high refractive index,[14,15] have attracted less attention than other materials. Hyodo *et al.* fabricated a H_2 sensor based on a Nb_2O_5 film coupled with Pd electrodes, which exhibited a fast and sensitive H_2 response at 100 °C.[16] Park *et al.* examined the sensing properties of Nb_2O_5-core/ZnO-shell nanorod sensors toward H_2 gas.[17] The response and recovery times of the Nb_2O_5-core/ZnO-shell nanorods at 10 000 ppm of H_2 at 300 °C were 17 and 23 s, respectively. Nevertheless, the sensor has to operate at a high temperature, which results in poor selectivity because it has to respond to a number of reducing gases with relatively high sensitivities at such a high working temperature. Wang *et al.* reported a H_2 sensor based on Nb_2O_5 nanowires, which exhibited a response time of 1.67 min at room temperature (RT).[10] The RT response time is too long to be useful in practical applications, and may be due to the large amounts of junctions among the nanowires, which slow down the diffusion of gas molecules and increase the electron scattering.[18] Several attempts have been made to decrease the resistance and the response time of network sensors. The methods resulted in either an unavoidable increase in the fabrication cost or the formation of composite materials.[19] A facile approach is to grow a Nb_2O_5 1D nanostructure with a vertical architecture, which reduces the number of junctions within the structure, to optimize the sensitivity of the sensor. Towards this aim, the hydrothermal method has been recognized as a simple, inexpensive and low temperature method for the growth of single-crystalline oxide nanostructures.

In this work, well-crystallized Nb_2O_5 nanorod arrays were *in situ* grown on Nb foil using a one-step hydrothermal process. A hydrogen sensor was designed using the Nb_2O_5 nanorod arrays without any catalyst, and exhibited a highly-sensitive and selective hydrogen sensing performance at RT. Moreover, the mechanism of hydrogen sensing and performance enhancement was also discussed in detail.

[a]*School of Science, Jilin Institute of Chemical Technology, Jilin 132022, P. R. China*
[b]*Hubei Key Laboratory of Ferro & Piezoelectric Materials and Devices, Faculty of Physics and Electronic Sciences, Hubei University, Wuhan 430062, P. R. China. E-mail: huym@hubu.edu.cn*
[c]*Department of Architecture and Material Engineering, Hubei University of Education, Wuhan 430205, P. R. China. E-mail: gqibin@hue.edu.cn*

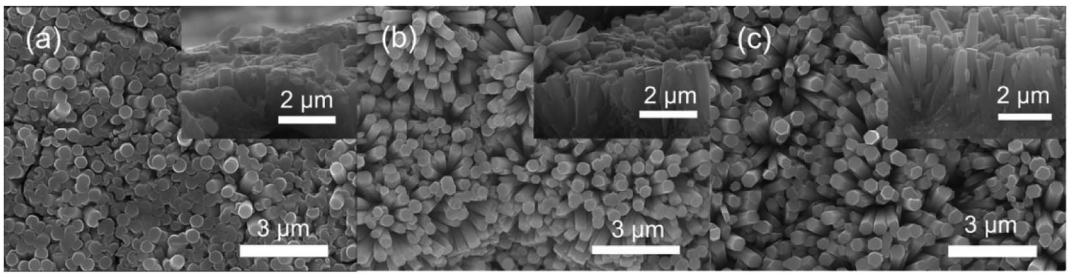

Fig. 1 SEM images of the as-prepared samples synthesized at different reaction temperatures, (a) 125 °C, (b) 150 °C, and (c) 175 °C. Inset: the corresponding cross-section SEM images.

Experimental

Synthesis and characterization

The growth of the Nb_2O_5 nanorod arrays has been reported in a previous work.[20] Nb_2O_5 nanorod arrays were *in situ* grown using a hydrothermal method on Nb foil, with 250 mm thick foil cut into 2 cm × 2 cm pieces. In a typical procedure, hydrogen peroxide was used as the oxidant mixed with deionized water in a 1 : 1 ratio. Then 0.5 g of NH_4F as the mineralizing agent was dissolved into the above mixture. Different hydrothermal temperatures were used from 125 °C to 175 °C. After hydrothermal reaction for 15 h, the samples were obtained.

The resultant nanorod phases were characterized using powder X-ray diffraction (PXRD Bruker D8A25, CuK, $\lambda = 1.5406$ Å). The morphologies and microstructures were examined using field-emission scanning electron microscopy (FESEM, JOEL JSM-7100F) and high-resolution transmission electron microscopy (HRTEM, JEOL Model JEM-2010).

Hydrogen sensing measurements

A sensor was fabricated by depositing a pair of Pt electrodes with a thickness of 100 nm on the surface of the nanorod arrays using a DC magnetron sputtering technique. Hydrogen sensing measurements were performed on a homemade measuring system at room temperature. The assembled gas test set-up consisted of two stainless steel chambers. During the testing process, the sensor was located at the center of the testing chamber and the target gases with different concentrations of H_2 were prepared in a mixing chamber. The concentration of H_2 could be precisely adjusted by controlling the flow rate and injection time of the gases to the testing chamber using mass flow controllers and electromagnetic valves. The sensor was connected to a digital multimeter (Keithley 2400) controlled by a computer to record the change of the resistance. Following the response process, the recovery properties were tested by removal of the H_2 gas with air. In this study, we determine the sensing properties of the Nb_2O_5 nanorod-based sensor for 1000–6000 ppm of hydrogen and its selectivity in environments of C_2H_6O, CO and NH_3.

Results and discussion

Materials characterization

The SEM images of the assembled Nb_2O_5 samples are presented in Fig. 1. It can be seen that the nanorods have uniform diameters, which are about 400 nm for all of the samples. According to the inset cross-section views, the samples form a buffer layer between the Nb foil and the Nb_2O_5 nanorods. The rod densities are 5.3×10^9, 4.5×10^9 and 3.9×10^9 rods per cm^2 corresponding to the samples prepared at 125 °C, 150 °C and 175 °C, respectively. The reduction in density means that there is a large spacing between the rods, which is beneficial for the hydrogen response. As shown in Fig. 1(a), the sample obtained at 125 °C consists of a large amount of columnar crystals. This sample is similar to the membrane because the spacing between the nanorods is small. In the case of the samples prepared at 150 °C and 175 °C, they both feature a lot of nanorods, but the length of the nanorods is increased in the 175 °C sample. From the cross-sectional image in Fig. 1(c), the nanorods have a length of 2 μm and are vertically oriented on the Nb substrate. The aspect ratio is 5 for the sample prepared at 175 °C, which is twice that for the sample prepared at 150 °C. This indicates that a higher hydrothermal temperature promotes the oriented growth of Nb_2O_5 nanorods.

The TEM image and selected area electron diffraction (SAED) pattern of an individual Nb_2O_5 nanorod obtained at 175 °C are shown in Fig. 2(a). The surfaces of the nanorod are smooth and pure. The cross-sectional width is 234 ± 20 nm and the length is 702 ± 128 nm. The SAED pattern shown in the inset demonstrates the single-crystalline nature of the hexagonal phase. The distinct lattice stripes can be clearly seen in the HRTEM image shown in Fig. 2(b). The calculated interlayer distances of (001) and (100) planes are 0.39 and 0.31 nm, which are in good agreement with the theoretical values for hexagonal Nb_2O_5 and indicate that [001] is the preferred growth direction.

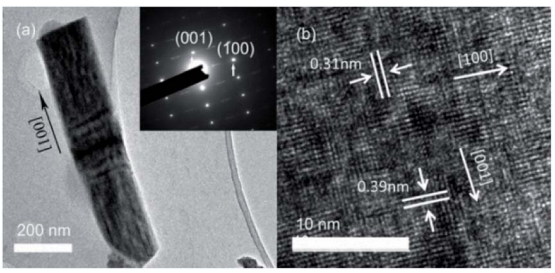

Fig. 2 The microstructure of a single Nb_2O_5 nanorod obtained at 175 °C. (a) The TEM image and SAED pattern (inset); (b) the HRTEM image.

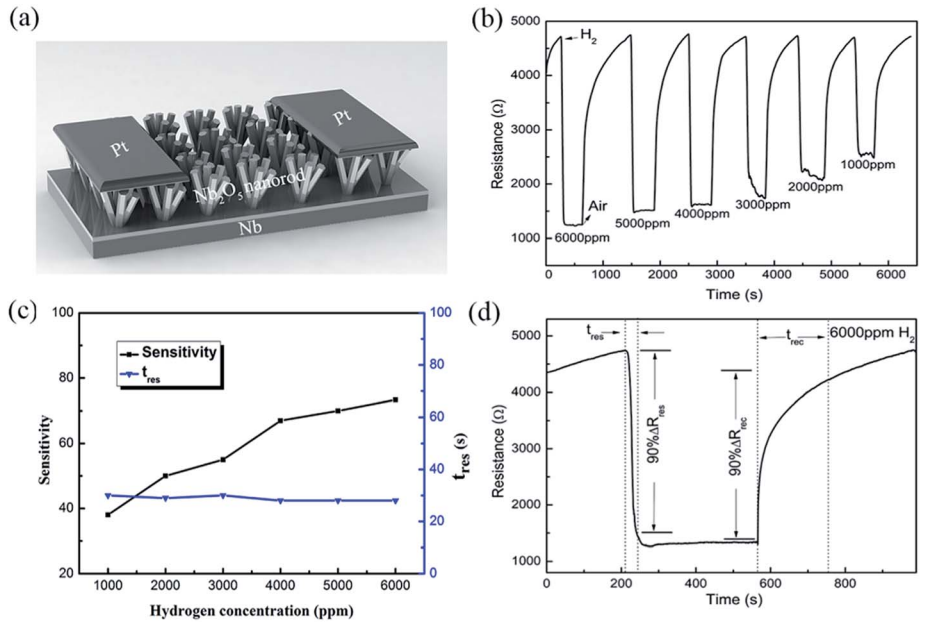

Fig. 3 Hydrogen response of the sample prepared at 175 °C measured at RT. (a) Schematic illustration of the fabricated sensor; (b) dynamic response resistances to the different concentrations of H_2; (c) H_2 concentration-dependent sensitivity and t_{res} of the Nb_2O_5 nanorod sensor; (d) dynamic response of the Nb_2O_5 sensor toward 6000 ppm of H_2.

RT hydrogen sensing performance

Fig. 3(a) shows a schematic diagram of the sensor made up of Nb_2O_5 nanorod arrays with Pt electrodes, based on the sample prepared at 175 °C. In this work, we define three physical parameters for studying the hydrogen sensing performance. The gas response sensitivity factor (S) is defined as the relative variation of the resistance, $S = (R_a - R_g)/R_a$, where R_a and R_g are the resistance of the sensor in air and in the target gas, respectively. The response time (t_{res}) and recovery time (t_{rec}) are defined as the time for the sensor to reach 90% of the final response and recovery, respectively. Fig. 3(b and c) show the responses of the sensor to hydrogen concentrations varying from 1000 to 6000 ppm. It can be seen that the Nb_2O_5 nanorod arrays have excellent hydrogen sensing properties at RT. The response sensitivity increases upon an increase in the hydrogen concentration, with a maximum sensitivity of 73.4% for 6000 ppm of H_2. The response time shows no obvious change, which may be due to the saturation of the adsorbed hydrogen that corresponds to the specific surface area. Fig. 3(d) shows the RT transient response of the Nb_2O_5 sensor under exposure to 6000 ppm of H_2 in air. Upon exposure to H_2 gas, the resistance of the sensor decreased rapidly and reached a minimum. It then recovered slowly to the initial resistance after pumping of the H_2 gas and flowing of air. This means that the sensor exhibited a fast and highly sensitive hydrogen response with t_{res} and t_{rec} values of 28 and 510 s, respectively. The recovery process was relatively slow, which may be due to the hydrogen removing process of the apparatus.

Table 1 lists the response times of the reported hydrogen sensors with Nb_2O_5 nanostructures. In comparison, the as-fabricated hydrogen sensor based on the Nb_2O_5 nanorod arrays exhibited an ideal hydrogen response at RT. The response time to 6000 ppm of H_2 is 28 s, which is shorter than that of a 2D nanofilm[16] and 1D nanowire[10] based sensor. Although the response time for our Nb_2O_5 nanorod array sensor is close to that of a Nb_2O_5-core/ZnO-shell nanorod based nanosensor,[17] the advantages of the current system are that it can be prepared using a simple synthesis process and the nanorods have not been decorated. The low cost makes it more commercially viable for room-temperature hydrogen sensing devices.

The most quoted model for explaining the hydrogen sensing mechanism of metal oxide semiconductors is the depletion layer modulation theory.[21]Fig. 4 shows a schematic illustration of the response and recovery processes of the Nb_2O_5 nanorod arrays.[22] As shown in Fig. 4(a), oxygen molecules are adsorbed onto the Nb_2O_5 nanorod surface in air and form oxygen ions by trapping electrons from the conduction band of Nb_2O_5, as expressed in the following equations:

$$O_2(g) \leftrightarrow O_2(ad) \quad (1)$$

$$O_2(ad) + e^- \leftrightarrow O_2^-(ad) \quad (2)$$

$$O_2(ad) + 2e^- \leftrightarrow 2O^-(ad) \quad (3)$$

This causes electron depletion at the surface and tends to increase the resistance, since Nb_2O_5 is an n-type semiconductor. It is necessary to point out that the types of the chemisorbed oxygen species depend on the temperature.[23] At low temperature, O_2^- is usually chemisorbed. Therefore, upon exposure to a hydrogen atmosphere (Fig. 4(b)), a higher concentration of O_2^- species reacts with the hydrogen molecules producing water and electrons at room temperature:

Table 1 A comparison of response times for different hydrogen sensors with Nb_2O_5 nanostructures

Materials	H_2 conc. (ppm)	t_{res} (s)	Temp. (°C)	Ref.
Nb_2O_5 nanofilm	8000	420	100	16
Nb_2O_5 nanowires	2000	100	RT	10
Nb_2O_5-core/ ZnO-shell nanorods	5000	24	300	17
Nb_2O_5 nanorod arrays	6000	28	RT	This work

$$2H_2 + O_2^-(ad) \rightarrow 2H_2O + 2e^- \quad (4)$$

This reaction is exothermic and the H_2O molecules desorb from the surface, while the electrons are released back to the Nb_2O_5 nanorods, thus decreasing the resistance. When the sensor is exposed to air again, the depletion layer width increases by adsorbing oxygen species, as shown in eqn (1) and (2). The resistance recovers to its initial level. In a practical environment, competition between these oxygen-removing electrons and the hydrogen gas restores these electrons. The steady state value of the resistance will depend on the hydrogen gas concentration because the concentration of oxygen is relatively constant.

Another component of the H_2 sensitivity is the dissociative chemisorption of hydrogen on the Nb_2O_5 nanorod surface. According to previous reports, chemisorbed hydrogen on oxide surfaces is more often observed in experiments.[24] During chemisorption, hydrogen acts in a surface state and produces an energy level for the transfer of charge from hydrogen to the conduction band of Nb. Therefore, an electron accumulation layer is created on the Nb_2O_5 nanorod surface that enhances its conductivity. When removing the ambient hydrogen using air, electron transfer takes place back to hydrogen and it desorbs. Thus, the accumulated layer of electrons disappears, and restores the original resistance of the Nb_2O_5 nanorod. The associated reaction is rapid and reversible at room temperature.

Moreover, the possible H_2 sensitivity is related to defects such as oxygen vacancies, which serve as adsorption sites for gas species. It has been found that hydrogen molecules can bind more tightly with oxygen vacancies to increase the conductivity.[23] This process is very slow at room temperature and leads to incomplete recovery.[25] Therefore, the defect-related hydrogen response may not be the major mechanism of the fast hydrogen response.

The high sensitivity of our sensor can be attributed to the high aspect ratio of the Nb_2O_5 nanorods because the high aspect ratio increases the contact area to the ambient. Therefore, the Nb_2O_5 nanorod array hydrogen sensor exhibits a fast and sensitive hydrogen response performance comparing with that of the Nb_2O_5 film-based sensor. However, the aspect ratio of the nanowires is larger than that of the nanorods, but the response time of the device based on the nanowire net is not faster than that of our sensor, because the nanowire net contains junctions, which leads to the internal diffusion resistance of chemisorbed oxygen ions.[18] This means that the net carrier density decreases with more junctions in the sensor, leading to a lengthening of the response time. The Nb_2O_5 nanorod arrays grown with vertical rods on the Nb substrate, moreover, the designed structure of the sensor, resulted in a current along the nanorods, that connected them to the Nb foil. As a result, by reducing the number of junctions and the oxygen ion diffusion resistance, the response time of the sensor based on Nb_2O_5 nanorod arrays was improved.

Fig. 5(a) shows five continuous response cycles to 6000 ppm of H_2, suggesting the outstanding repeatability of this sensor. Moreover, the gas selectivity to H_2 was also examined in contrast with C_2H_6O, CO and NH_3 for this Nb_2O_5 nanorod array hydrogen sensor. As shown in Fig. 5(b), the sensing response to H_2 gas was stronger than that of the other gases, suggesting that the sensor has excellent selectivity for H_2 gas. This can be attributed to the highly reducing behaviour of the H_2 gas. However, the sensor shows low sensitivities for other reducing gases, such as C_2H_6O, CO and NH_3. Although the exact reason for this is not very clear at present, it is proposed that the molecular size may be responsible for the selectivity.[26] The diameters of the C_2H_6O and NH_3 molecules are much larger than those of H_2 and CO. It is difficult for the larger molecules to diffuse into the inner layer of the nanorod arrays and react with the chemisorbed oxygen. Moreover, the bond energy of H_2 (436 kJ mol^{-1}) is much lower than that of CO (1072 kJ mol^{-1}). Hence, it is easier to destroy the bond in H_2 at a lower temperature. As a result, the Nb_2O_5 nanorod arrays exhibit a higher response to hydrogen against C_2H_6O, CO and NH_3.

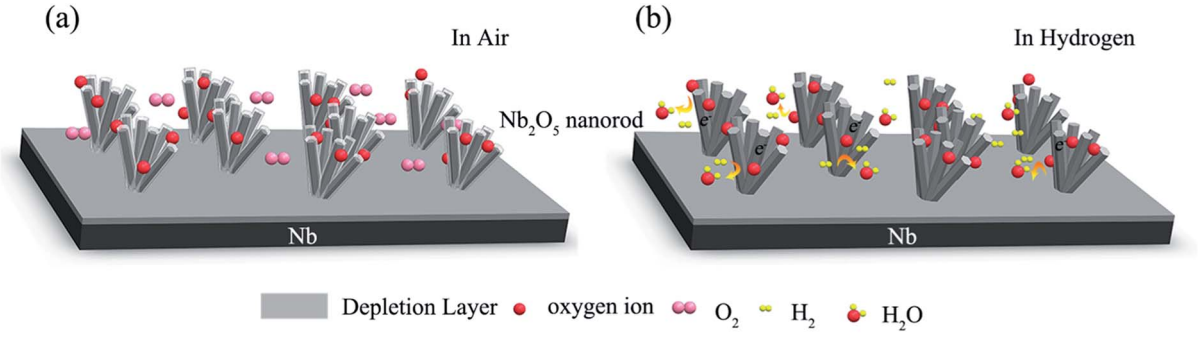

Fig. 4 Schematic diagram of the H_2 sensing mechanism of the Nb_2O_5 nanorod arrays.

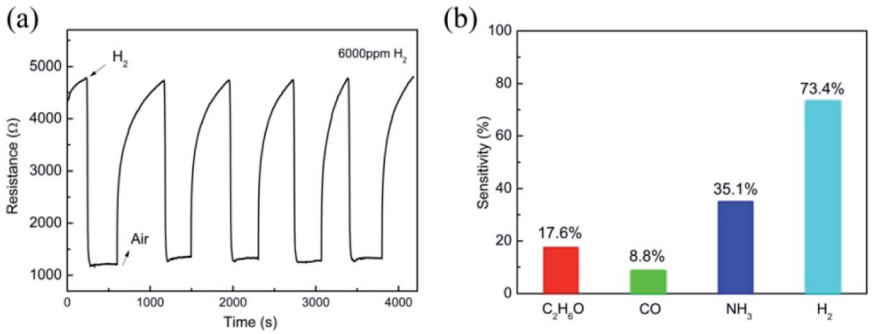

Fig. 5 (a) Five response cycles to 6000 ppm of H_2; (b) the gas response to different gases.

Conclusions

Nb_2O_5 nanorod arrays with a hexagonal phase were *in situ* grown *via* a facile hydrothermal route at 175 °C, and a hydrogen sensor based on Nb_2O_5 nanorod arrays was prepared. The aspect ratio of the Nb_2O_5 nanorods was 5 and the arrays have a suitable spacing, which allows more gas molecules to adsorb on them. The decreased number of junctions between the vertical nanorod arrays makes it easier for chemisorbed oxygen ions to diffuse, resulting in a highly sensitive and selective hydrogen sensor. A sensitivity of 74.3% and response time of 28 s toward 6000 ppm of H_2 at room temperature were achieved. The response time is satisfactory when considering that the surface has not been functionalized using a catalyst and the nanorods have not been doped. The major hydrogen sensing mechanism is the redox reaction between the H_2 and chemisorbed oxygen species. Our device has potential for use as a practical highly-sensitive, low-cost hydrogen sensor at room temperature.

Conflicts of interest

There are no conflicts to declare.

Acknowledgements

This work was financially supported by the National Natural Science Foundation of China (Grant No. 61274073, 11474088, 11504099) and the Science and Technology Department of Hubei Province (Grant No. 2016AAA002, 2016CFA081, 2013CFB014).

References

1 W. J. Buttner, M. B. Post, R. Burgess and C. Rivkin, *Int. J. Hydrogen Energy*, 2011, **36**, 2462.
2 T. Hübert, L. Boon-Brett, G. Black and U. Banach, *Sens. Actuators, B*, 2011, **157**, 329.
3 O. Lupan, V. V. Ursaki, G. Chai, L. Chow, G. A. Emelchenko, I. M. Tiginyanu, A. N. Gruzintsev and A. N. Redkin, *Sens. Actuators, B*, 2010, **144**, 56.
4 Y. Li, X. Yu and Q. Yang, *J. Sens.*, 2009, **2009**, 402174.
5 J. Lee, D. H. Kim, S. H. Hong and J. Y. Jho, *Sens. Actuators, B*, 2011, **160**, 1494.
6 L. L Fields, J. P. Zheng, Y. Cheng and P. Xiong, *Appl. Phys. Lett.*, 2006, **88**, 263102.
7 J. M. Lee, J. Park, S. Kim, S. Kim, E. Lee, S. J. Kim and W. Lee, *Int. J. Hydrogen Energy*, 2010, **35**, 12568.
8 M. A. Andio, P. N. Browning, P. A. Morris and S. A. Akbar, *Sens. Actuators, B*, 2012, **165**, 13.
9 S. S. Arbuj, R. R. Hawaldar, U. P. Mulik and D. P. Amalnerkar, *J. Nanoeng. Nanomanuf.*, 2013, **3**, 79.
10 Z. Wang, Y. Hu, W. Wang, X. Zhang, B. Wang, H. Tian, Y. Wang, J. Guan and H. Gu, *Int. J. Hydrogen Energy*, 2012, **37**, 4526.
11 R. A. Rani, A. S. Zoolfakar, J. Z. Ou, M. R. Field, M. Austin and K. Kalantar-zadeh, *Sens. Actuators, B*, 2013, **176**, 149.
12 M. Schmitta, S. Heusinga, M. A. Aegertera, A. Pawlickab and C. Avellanedab, *Sol. Energy Mater. Sol. Cells*, 1998, **54**, 9.
13 S. R. Yu, X. P. Zhang, Z. M. He, Y. H. Liu and Z. H. Liu, *J. Mater. Sci.*, 2004, **15**, 687.
14 X. Xiao, G. Dong, C. Xu, H. He, H. Qi, Z. Fan and J. Shao, *Appl. Surf. Sci.*, 2008, **255**, 2192.
15 A. Le Viet, R. Jose, M. V. Reddy, B. V. R. Chowdari and S. Ramakrishna, *J. Phys. Chem. C*, 2010, **114**, 21795.
16 T. Hyodo, J. Ohoka, Y. Shimizu and M. Egashira, *Sens. Actuators, B*, 2006, **117**, 359.
17 S. Park, S. Part, S. Lee, H. W. Kim and C. Lee, *Sens. Actuators, B*, 2014, **202**, 840.
18 S. Yang, Z. Wang, Y. Zou, X. Luo, X. Pan, X. Zhang, Y. Hu, K. Chen, Z. Huang, S. Wang, K. Zhang and H. Gu, *Sens. Actuators, B*, 2017, **248**, 160.
19 S. Park, H. Kheel, G. J. Sun, H. W. Kim, T. Ko and C. Lee, *Met. Mater. Int.*, 2016, **22**, 730.
20 J. He, Y. Hu, Z. Wang, W. Lu, S. Yang, G. Wu, Y. Wang, S. Wang, H. Gu and J. Wang, *J. Mater. Chem. C*, 2014, **2**, 8185.
21 H. Gu, Z. Wang and Y. Hu, *Sensors*, 2012, **12**, 5517.
22 J. Zhang, X. Liu, G. Neri and N. Pinna, *Adv. Mater.*, 2016, **28**, 795.
23 O. Lupan, V. V. Ursaki, G. Chai, L. Chow, G. A. Emelchenko, I. M. Tiginyanu, A. N. Gruzintsev and A. N. Redkin, *Sens. Actuators, B*, 2010, **144**, 56.
24 Z. L. Wang and J. Nanosci, *Nanotechnology*, 2008, **8**, 27.
25 O. K. Varghese, D. Gong, M. Paulose, K. G. ong and C. A. Grimes, *Sens. Actuators, B*, 2003, **93**, 338.
26 A. Katsuki and K. Fukui, *Sens. Actuators, B*, 1998, **52**, 30.